GEOPHYSICS, VOL. 68, NO. 6 (NOVEMBER-DECEMBER 2003); P. 1822–1834, 16 FIGS., 1 TABLE.
10.1190/1.1635035

Velocity-porosity relationships, 1: Accurate velocity model for clean consolidated sandstones

Mark A. Knackstedt*, Christoph H. Arns*, and W. Val Pinczewski‡

ABSTRACT

We use numerical simulations to derive the elastic properties of model monomineralic consolidated sandstones. The model morphology is based on overlapping spheres of a mineral phase. We consider model quartzose and feldspathic sands. We generate moduli-porosity relationships for both the dry and water-saturated states. The ability to control pore space structure and mineralogy results in numerical data sets which exhibit much less noise than corresponding experimental data. The numerical data allows us to quantitatively analyze the effects of porosity and the properties of the mineral phase on the elastic properties of porous rocks. The agreement between the numerical results and available experimental data for clean consolidated sandstones is encouraging.

We compare our numerical data to commonly used theoretical and empirical moduli-porosity relationships. The self-consistent method gives the best theoretical fit to the numerical data. We find that the empirical relationship of Krief et al. is successful at describing the numerical data for dry shear modulus and that the recent empirical method of Arns et al. gives a good match to the numerical data for Poisson's ratio or V_p/V_s ratio of dry rock. The Raymer equation is the best of the velocity-porosity models for the water-saturated systems. Gassmann's relations are shown to accurately map between the dry and fluid-saturated states.

Based on these results, we propose a new empirical method, based solely on a knowledge of the mineral modulus, to estimate the full velocity-porosity relationship for monomineralic consolidated sands under dry and fluid-saturated states. The method uses the equation of Krief et al. for the dry shear modulus and the empirical equation of Arns et al. for the dry Poisson's ratio. Gassmann's relations are applied to obtain the fluid-saturated states. The agreement between the new empirical method, the numerical data and available experimental data for dry and water-saturated states is encouraging.

INTRODUCTION

Accurate elastic modulus-porosity or velocity-porosity relationships are critical to the determination of lithology from seismic or sonic log data as well as for direct seismic identification of pore fluids. Existing predictive methods reduce to two simple elements: establish empirical relationships between elastic moduli and porosity for a reference fluid (usually water), and then use Gassmann's relations to map these to other pore fluid states. Unfortunately, experimental modulus-porosity data usually display considerable scatter. The scatter is primarily due to variations in microstructure (pore shape, size, degree of compaction) (Marion et al., 1992) as well as clay content and distribution (Han, 1986) and the presence of cracks within the matrix. These features, which are difficult to measure quantitatively, comprise the microstructure of the rock. In order to predict realistic rock properties or to properly interpret experimentally measured modulus-porosity relationships, it is necessary to have an accurate method of relating elastic properties to porosity, mineralogy and microstructure. Existing theoretical methods [e.g., bounds (Hashin and Shtrikman, 1963) and effective medium theories (Budiansky, 1965; Hill, 1965; Berryman, 1992; Gubernatis and Krumsahl, 1975; Korringa et al., 1979)] are based on different assumptions and choice of reference states, and often result in different predictions. Moreover, they provide limited insight into the effects of complex microstructure and mineralogy on velocity-porosity relationships.

It is now possible to accurately estimate the elastic properties of complex materials from computations made directly

Manuscript received by the Editor January 18, 2002; revised manuscript received October 28, 2002.
*Australian National University, Department of Applied Mathematics, Research School of Physical Sciences and Engineering, Canberra ACT 0200, Australia. E-mail: mark.knackstedt@anu.edu.au; christoph.arns@anu.edu.au.
‡University of New South Wales, School of Petroleum Engineering, Sydney, NSW 2052, Australia. E-mail: v.pinczewski@unsw.edu.au.

on digitized 3D images of rock microstructure (Arns et al., 2002b) or on statistically equivalent model microstructures (Arns et al., 2002a). These techniques offer the possibilities of exploring, for the first time, velocity-to-porosity transformations in a more controlled environment than is possible experimentally and of providing greater insight and better predictive power than is possible with existing analytical models. In this paper, we mimic the microstructure of consolidated sandstones with a morphology based on overlapping grains, and computationally generate modulus-porosity relationships for both the dry and water-saturated states. We consider both model quartzose and feldspathic sands, and compare our results with existing theoretical and empirical relationships for deriving moduli-porosity estimates. The self-consistent method (Budiansky, 1965; Hill, 1965; Gubernatis and Krumsahl, 1975; Korringa et al., 1979) gives the best theoretical fit to the numerical data. We note that the Krief empirical relationship (Krief et al., 1990) is particularly successful at describing the numerical data for dry shear modulus, and a recently derived method (Arns et al., 2002a) gives a good prediction of the Poisson's ratio data for dry rock. We find that the Raymer equation (Raymer et al., 1980) is the best of the simple modulus-porosity models for water-saturated cases. In all cases Gassmann's relations accurately map between the dry and fluid-saturated states.

Based on these results, we propose an accurate empirical method for estimating the full modulus/porosity relationship for well-consolidated sands from only a knowledge of the mineral content of the rock. A two-step process is described:

1) Estimate dry velocity-porosity relationship via Krief et al.'s (1990) and Arns et al.'s (2002a) equations.
2) Apply Gassmann's relations to obtain fluid-saturated states.

The match to numerical data, available experimental data, and empirical fits to experimental data for clean sands is good.

METHODS

Mineral phase microstructure

A natural model for a consolidated sandstone is based on overlapping spheres or grains (OS model). The model is generated by randomly placing solid (discretized) spheres in a cubic cell to produce a set of overlapping grains. The space outside the grains is the pore space with porosity ϕ. The pore phase is macroscopically connected above porosities of $\simeq 4\%$, and the solid phase remains connected to very high porosity. We use the model to calculate elastic properties over a very wide range of porosity: $5\% < \phi < 50\%$. To generate the microstructure we choose solid spheres of (discretized) radius r voxels in a cubic box of size $10 \times r$ voxels. In Figure 1, we illustrate the microstructure of the pore space of the model at a number of different porosities.

Although it is possible to formulate more realistic models which include the effects of consolidation, compaction and cementation (Øren et al., 1998), the OS model has been shown to provide a very good match for the microstructure of Fontainebleau sandstone data (Thovert et al., 2001) without the heavy computational expense of more complex models. Moreover, we have compared the predictions of the elastic modulus of the OS model with the properties derived from digital 3D images of sandstones and from experiment (Han, 1986). The match is good across the full range of porosity measured (Arns et al., 2002b).

Elastic simulation

We use a finite-element method (FEM) to estimate the elastic properties of the model system. FEM uses a variational formulation of the linear elastic equations and finds the solution by minimizing the elastic energy using a fast conjugate-gradient method. Each voxel is taken to be a trilinear finite element. Details of the method and the programs can be found elsewhere (Garboczi and Day, 1995b; Garboczi, 1998). In principle, the

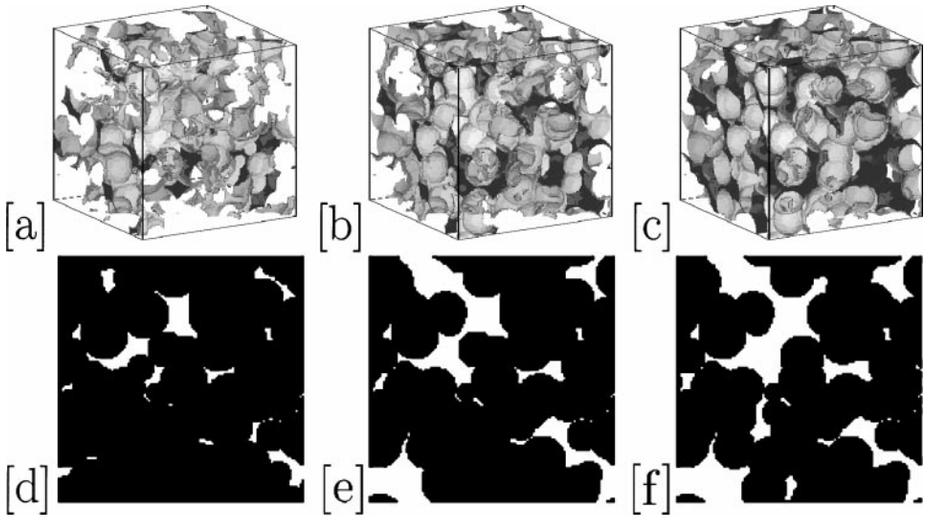

FIG. 1. Images of the pore space of an OS model. Three-dimensional pore space images of the model microstructure are shown at porosities of (a) 10%, (b) 20%, and (c) 30%. Two-dimensional slices through the 3D data sets are shown at (d) $\phi = 10\%$, (e) 20%, and (f) 30%. The image size is ten times the sphere radius.

method provides an exact solution to the equations of elasticity for a body subjected to a macroscopic strain. The resultant average stress in the body is used to calculate the various elastic moduli. In practice, the accuracy of the results are limited by discretization errors (how well a continuum model can be resolved) and statistical noise (limited system size) (Roberts and Garboczi, 2000; Arns et al., 2002b). A minimum of ten independent samples were used to reduce statistical errors to the order of a few percent. Discretization errors, which can remain of the order of 20% at high resolutions, are scaled out by generating the same microstructures for different resolutions (grain sizes) and extrapolating to infinite resolution; for details see Roberts and Garboczi (2000) and Arns et al. (2002b).

The elastic properties assigned to the mineral comprising the rock skeleton were taken from Mavko et al. (1998) and are summarized in Table 1. The choice of the water saturated condition is made to allow for comparison with the experimental data of Han (1986).

Table 1. Material properties for the minerals and water (40 MPa) used in the simulations (Mavko et al., 1998). *K* is the bulk modulus, μ the shear modulus, and ρ the rock density. The water conditions are chosen to allow for comparison with experimental data (Han, 1986).

Material	K (GPa)	μ (GPa)	ρ (g/cm^{-3})
Quartz	37.0	44.0	2.65
Feldspar	37.5	15.0	2.62
Water ($T = 200^{\circ}$C, 40 MPa)	2.2	0.0	1.00

RESULTS

Dry rock

Figure 2 shows results for the dry bulk modulus K, shear modulus μ, V_p, and V_p/V_s ratio for the OS model as a function of porosity for two different simple (single-mineral) phases of quartz and feldspar. The moduli of the rocks trend between the modulus of the mineral at low porosities to zero at higher porosities. Although the bulk modulus of quartz (37.0 GPa) and feldspar (37.5 GPa) are very similar, the curve for the bulk modulus of the porous systems vary appreciably. Moreover, although $K_{\text{feld}} > K_{\text{quartz}}$, the curves for feldspar are consistently lower than those for the quartz. The V_p curve is approximately linear with porosity for both mineral phases, and the V_p/V_s ratio exhibits a strong dependence on porosity and tends towards a fixed point $(V_p/V_s)^* \simeq 1.63 = \sqrt{(8/3)}$ at higher porosities. This behavior was noted previously (Arns et al., 2002a) and corresponds to a fixed point in the Poisson's ratio $\nu^* = 0.2$. The behavior is similar to that predicted in two dimensions (Day et al., 1992).

In comparison with typical experimental results [see e.g., Han (1986)], the computations display a notable lack of noise or scatter. This is primarily due to the elimination of the many factors exhibited by experimental samples (variations in clay content and presence of cracks) within the model microstructure. The standard error in the computed data (shown in the Figure 2) is extremely small: <1% for most of the numerical measurements. Only for V_p/V_s at high porosities does the standard error exceed a few percent. For systems at higher porosity,

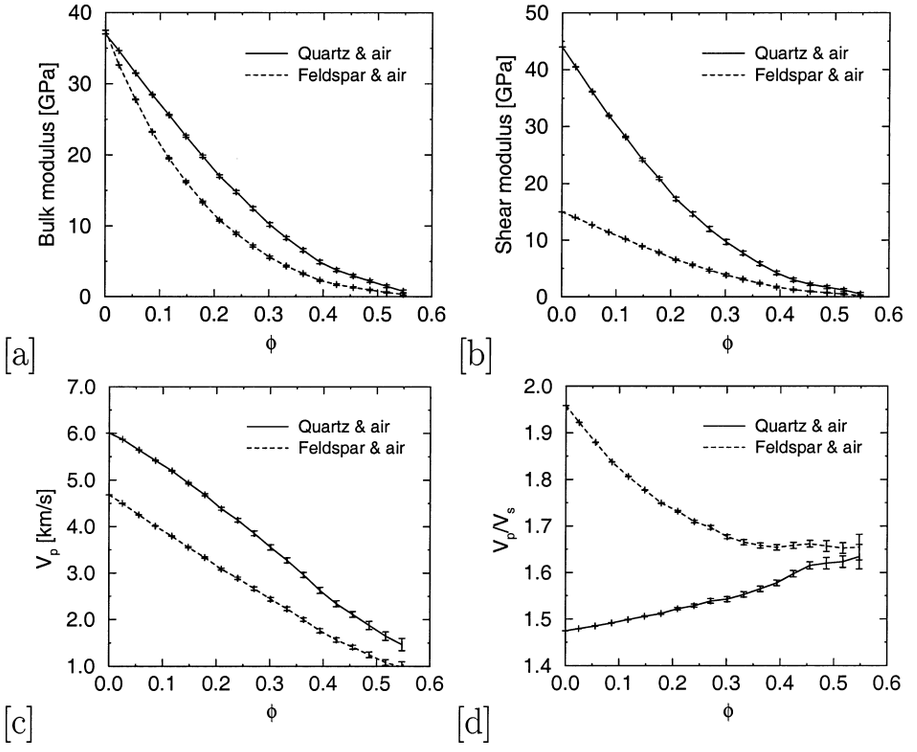

FIG. 2. Results of the simulation for the variation of the (a) bulk modulus, (b) shear modulus, (c) V_p, and (d) V_p/V_s ratio under dry conditions as a function of porosity for the single-phase OS model with quartz and feldspar as the mineral phase.

the elastic properties become more dependent on small tenuous connections, which are increasingly difficult to resolve numerically and, therefore, larger statistical errors are observed. Importantly, the numerical data in the region of most practical interest for consolidated rock, $5\% < \phi < 30\%$, exhibits markedly less noise than typical experimental data. This allows us to quantitatively analyze the effects of porosity and the elastic properties of the mineral phase on (effective) elastic properties. In a later section, we use this numerical data to test common empirical and theoretical models used to predict the elastic properties of sedimentary rocks.

Water-saturated rock

In Figure 3, we show results for the water-saturated values of the bulk modulus K, shear modulus μ, V_p, and V_p/V_s ratio for the OS model as a function of porosity for the two different single-mineral phases. Again, despite the bulk modulus of quartz and feldspar being very similar, the curves for the bulk modulus of the water-saturated porous systems differ appreciably. The bulk modulus trends between the modulus of the mineral at zero porosity to values corresponding to a mineral-pore suspension at large ϕ (Nur et al., 1991, 1995). The shear modulus for the saturated system exhibits the same behavior as the dry rock, going to zero at higher porosities. The V_p curves are approximately linear with porosity for both mineral phases. The V_p/V_s ratio exhibits a strong dependence on mineralogy. The quartz data shows a slow linear increase with porosity with a slow divergence. The feldspar data exhibits an approximately constant region for $0 < \phi < 0.3$ with a strong divergence for $\phi > 0.3$.

Comparison with Gassmann's relations

The low-frequency Gassmann's equations relate the bulk and shear moduli of a saturated porous medium to the moduli of the same medium in a drained (dry) state. For an isotropic, monomineralic medium, Gassmann's relations allow the effective bulk modulus K_{sat} of the saturated rock to be calculated from a knowledge of the dry frame modulus K_{dry}, the solid matrix modulus K_s, and the pore fluid modulus K_f:

$$\frac{K_{sat}}{K_s - K_{sat}} = \frac{K_{dry}}{K_s - K_{dry}} + \frac{K_f}{\phi(K_s - K_f)}. \qquad (1)$$

Gassmann's relations show that the shear modulus is mechanically independent of the properties of any fluid present in the pore space:

$$\mu_{dry} = \mu_{sat}. \qquad (2)$$

Gassmann's relations [equations (1)–(2)] assume that the porous medium contains only one type of solid constituent with a homogeneous mineral modulus and that the pore space is statistically isotropic and is valid for quasistatic conditions (i.e., at sufficiently low frequencies such that the induced pore pressures are in equilibrium throughout the pore space). This limit coincides with the conditions simulated with the finite-element approach. The results summarized in Figure 4 show that the numerical data for the OS model indeed obeys Gassmann's equations. The numerical prediction for both the bulk and shear modulus are in excellent agreement with Gassmann's equations. The match to Gassmann's relations provides further verification of the accuracy of the numerical results.

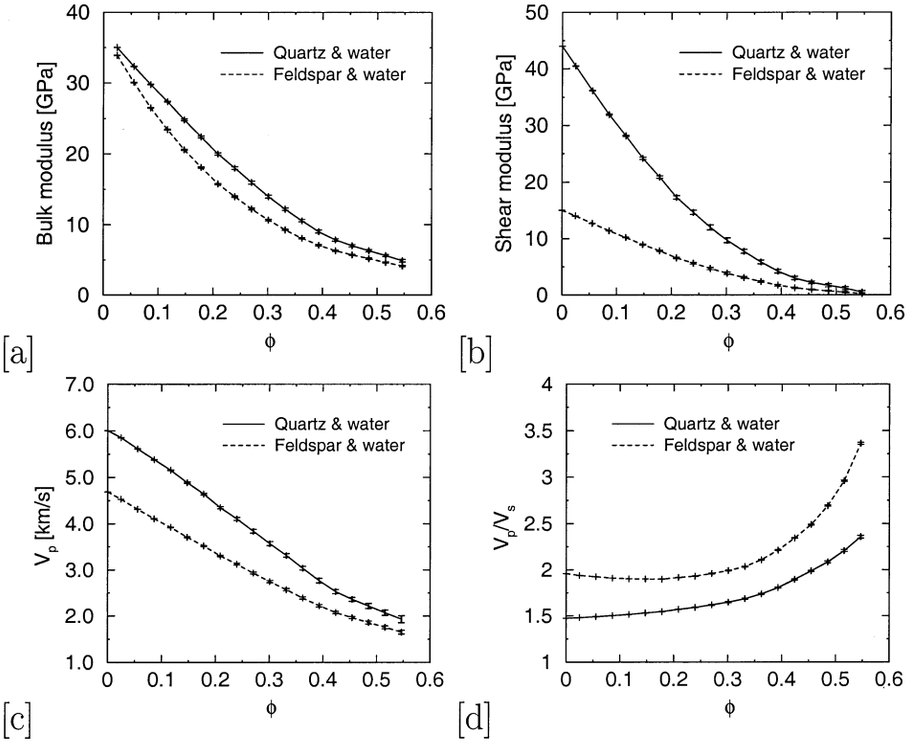

FIG. 3. Results of the simulation for the variation of the (a) bulk modulus, (b) shear modulus, (c) V_p, and (d) V_p/V_s ratio under water-saturated conditions as a function of porosity for the single-phase OS model with quartz and feldspar as the mineral phase.

Comparison to experiment

We compare the computed bulk and shear modulus for dry and water-saturated model quartz sandstone morphologies with experimentally mesured values (Han, 1986). Although these measurements were made at ultrasonic frequencies, Han (1986) suggests that the frequency dispersions a minimal; the Biot-dispersions are $\simeq$1% and the non-Biot dispersions negligible for clean sandstones.

Dry rock.—Han (1986) reports a number of velocity measurements for dry clean quartz sandstones. The numerical data for the simulations on the quartz OS morphology is compared to these measurements in Figure 5. The match between the numerical calculations and experimental measurements is encouraging, and suggests that the simulation on the model granular morphology provides a reasonable representation of consolidated sandstone structure.

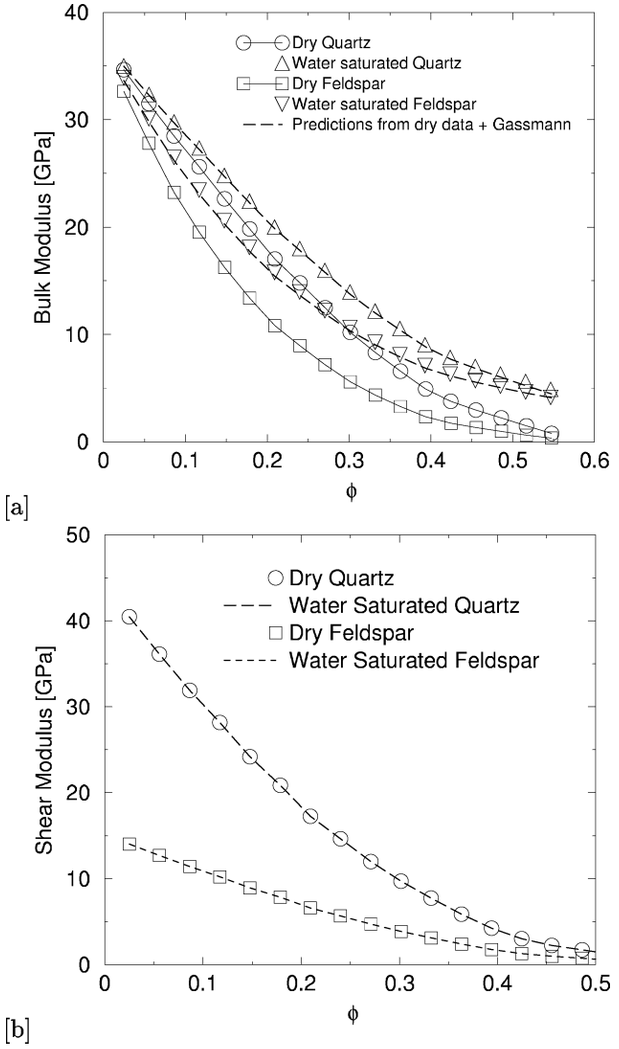

FIG. 4. Comparison of the results of the simulations for dry and water-saturated OS models to Gassmann prediction based on the dry rock data with their standard errors. In (a), we give the numerical results for the dry rock data and show best fits to the data points (solid lines). We use these fits and equation (1) to predict the values of the water-saturated curves (dotted curves). We also show the numerical predictions for the water-saturated results. The fit to the Gassmann's equations is excellent. In [b], we show that the shear modulus is independent of the pore fluid equation (2).

Water-saturated rock.—Han (1986) provided empirical equations to describe measured velocities for water-saturated clean sandstones as a function of porosity:

$$V_p = 6.08 - 8.06\phi \text{ km/s}, \tag{3}$$

$$V_s = 4.06 - 6.28\phi \text{ km/s}. \tag{4}$$

Comparisons between the numerical data for the quartz OS model and the empirical equations are shown in Figure 6. The agreement, over such a large range of porosities, is excellent.

Empirical equations, based on crossplots of experimental data, are also used to relate V_p to V_s. Data for sandstones compiled by Castagna et al. (1993) is represented by

$$V_s = 0.804V_p - 0.856 \text{ km/s}. \tag{5}$$

Han (1986) presents an equation for sandstones with clay volume (<25%);

$$V_s = 0.754V_p - 0.657 \text{ km/s}. \tag{6}$$

Figure 7a shows a comparison between computed velocities and the empirical equations (5) and (6). The overall agreement is satisfactory but the numerical data falls slightly below the values given by the empirical relationships. A possible explanation for this is that the empirical relationships [equations (5) and (6)] include data from sandstones with significant proportions of clay. To illustrate that this could be the case, we plot in Figure 7b experimental data points for the saturated velocities of Han (1986) for clean sandstones, the prediction of Equation (6), and numerical data. The numerical predictions now give an excellent match to this experimental data for clean quartz sands.

COMPARISON TO VELOCITY-POROSITY MODELS

Dry rock

Theoretical models.—A number of theoretical methods have been proposed for estimating the properties of sedimentary rock. Bounding methods are rigorously based on microstructural information. Common bounds on the properties of a two-phase composite without specifying any geometric information beyond porosity are the Hashin-Shtrikman bounds (Hashin and Shtrikman, 1963). Higher order bounds can be derived (Milton, 1982), but the microstructural information needed to evaluate the results is not easy to obtain. Effective medium approaches (Hashin, 1983) have also been developed. We compare our numerical results to three of the most commonly cited theoretical methods: Hashin-Shtrikman bounds, the self-consistent method (SCM), and the differential effective medium (DEM) approach.

From a specification of the volume fraction and constituent moduli, one can obtain rigorous upper and lower bounds for the elastic moduli of any composite material. The so-called Hashin-Shtrickman bounds (Hashin and Shtrikman, 1962) are

given by

$$K_{HS}^{+} = K_s + \frac{\phi}{(K_f - K_s)^{-1} + (1-\phi)(K_s + 4/3\mu_s)^{-1}}, \quad (7)$$

$$\mu_{HS}^{+} = \mu_s + \frac{\phi}{(\mu_f - \mu_s)^{-1} + \dfrac{2(1-\phi)(K_s + 2\mu_s)}{5\mu_s(K_s + 4/3\mu_s)}}. \quad (8)$$

Upper and lower bounds are computed by interchanging the moduli of the solid and fluid components. In the case where one phase has zero elastic moduli, the lower bound becomes zero, and only the upper bound is useful.

One common effective medium theory, the DEM method is constructed by incrementally adding inclusions of one phase into the second phase with known constituent properties. DEM does not treat each constituent symmetrically, but defines a preferred host material. From the composite host medium $K^*_{DEM}(\phi)$ at some porosity value ϕ is known. One then treats $K^*_{DEM}(\phi)$ as the composite host medium and $K^*_{DEM}(\phi + d\phi)$ as the effective constant after a small proportion $d\phi/(1-\phi)$ of the composite host has been replaced by inclusions of the second phase. For a solid matrix host, the coupled system of ordinary differential equations for the moduli is given by Berryman (1992):

$$(1-\phi)\frac{d}{d\phi}[K^*(\phi)] = (K_f - K^*)P^*, \quad (9)$$

$$(1-\phi)\frac{d}{d\phi}[\mu^*(\phi)] = (\mu_f - \mu^*)Q^*, \quad (10)$$

with initial conditions $K^*(0) = K_s$ and $\mu^*(0) = \mu_s$, and where P^* and Q^* are shape-dependent geometric factors [see, e.g., Table 4.9.1 of Mavko et al. (1998)]. For the present study, we used the geometric factors for spherical inclusions. Although this is not realistic, it is unclear what shape one should use. Any simple convex inclusion shape does not accurately define the true morphology of the pore space.

In the SCM of Hill (1965) and Budiansky (1965), the host medium is assumed to be the composite itself. The equations of elasticity are solved for an inclusion embedded in a medium of unknown effective moduli. The effective moduli are then found by treating K_{scm}, μ_{scm} as tunable parameters. The result is given in general form (Berryman, 1980) as

$$\phi(K_f - K_{scm})P^{*fi} + (1-\phi)(K_s - K_{scm})P^{*si} = 0, \quad (11)$$

$$\phi(\mu_f - \mu_{scm})Q^{*fi} + (1-\phi)(\mu_s - \mu_{scm})Q^{*si} = 0. \quad (12)$$

where the indices to P and Q indicate the inclusions of fluid "$*fi$" and solid "$*si$" into a background medium of effective moduli K^* and μ^*. The solution for the effective bulk moduli is found iteratively. In the SCM study, we considered the geometric factors for spherical grains and pores only. The SCM

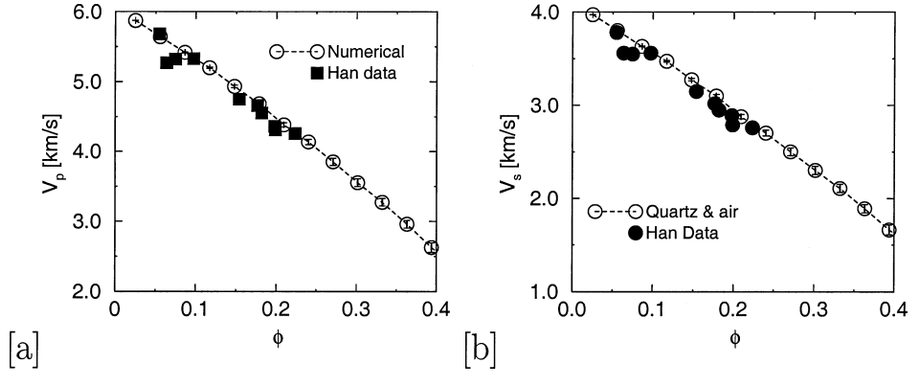

FIG. 5. Comparison of the results of the simulations for (a) V_p and (b) V_s of water-saturated sandstone to the dry velocity data of Han (1986) for clean sandstones.

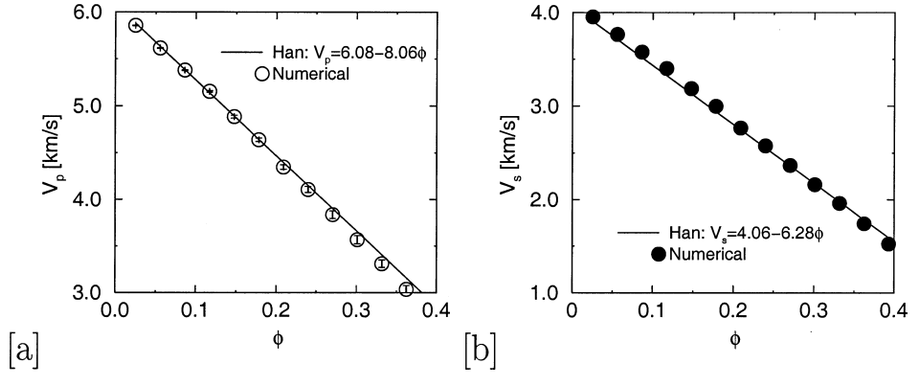

FIG. 6. Comparison of the results of the simulations for (a) V_p and (b) V_s of water-saturated sandstone to the empirical velocity-porosity equations derived by Han (1986) for clean sandstones. The match is excellent for all ϕ.

produces a single formula in which all components are treated uniformly, with no one material being distinguished as the host to the others. Such a symmetric formula has been thought to be more appropriate in complex aggregates like consolidated granular rocks, and was shown (Berge et al., 1993) to accurately predict the mechanical behavior of a sintered glass–bead pack.

We compare the above three theories to our numerical predictions in Figure 8. We note that none of the theoretical models provide a satisfactory fit to the OS model. The SCM theory gives a much better fit to the data than either the DEM or the Hashin-Shtrickman upper bound. This is consistent with the observations of Berge et al. (1993), who showed that the SCM more accurately predicts the elastic properties of consolidated granular media. Further, the SCM theory predicts a vanishing modulus for $\phi > 0.5$, which is similar to the empirical critical porosity model (Nur et al., 1995) discussed in the next section.

The conventional DEM model always predicts the percolation or critical porosity (where the system falls apart) at 0 and 100%. Mukerji et al. (1995) developed a modified DEM to incorporate a more realistic critical or percolation porosity. For sandstones, the critical porosity ϕ_c where the mineral grains no longer are load bearing is approximately $\phi_c = 40\%$. The modified DEM incorporates this percolation behavior in the predictions. The prediction with $\phi_c = 40\%$ is given also in Figure 8. We note that the modified DEM underestimates the numerical data.

It is interesting to note that both effective-medium theories based on spherical pores predict the same critical Poisson's ratio $\nu^* = 0.2$ ($V_p/V_s = \sqrt{8/3}$) (Garboczi and Day, 1995) as $\phi \to \phi_c$. The DEM predicts $\phi_c = 1$, whereas the SCM predicts $\phi_c = 0.5$, close to that observed in Figure 2d. Figure 9 shows a comparison between the Poisson's ratio predicted by the SCM theory and our numerical computations. Although the SCM prediction displays similar limiting behavior to the numerical data, the match is not consistent for both minerals, particularly for feldspathic sands.

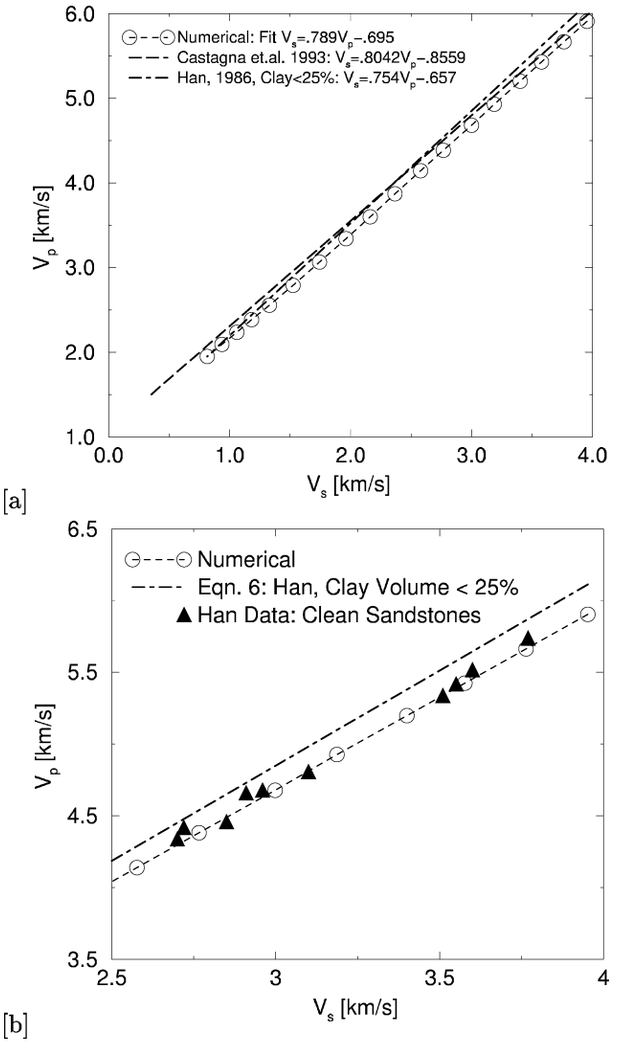

FIG. 7. (a) Comparison of the results of the simulations for water-saturated sandstone to the empirical equations of Han (1986) and Castagna et al. (1993). The numerical data is slightly below the two empirical curves, but exhibits the expected linear relationship between V_p and V_s. In (b), we show the experimental data of Han (1986) for clean sandstones and note that the numerical fit gives the best match to the data.

Empirical relationships.—Experimental measurements often show that relatively simple empirical relationships can sucessfully describe the properties of sedimentary rock. In this section, we compare a number of empirical equations with the numerical data discussed in the previous section.

If the dry rock is modelled as an elastic porous solid, the dry rock bulk modulus may be written as $K_{dry} = K_0(1-\beta)$, where β is Biot's coefficient. Krief et al. (1990) used experimental data to find an empirical relationship for β as a function of ϕ. The resultant expression is $(1-\beta) = (1-\phi)^{m(\phi)}$, where $m(\phi) = 3/(1-\phi)$. They also used the empirical result of Pickett (1963), which assumes that the dry rock Poisson's ratio is approximately equal to the mineral Poisson's ratio, $\mu_{dry}/K_{dry} = \mu_0/K_0$, which leads to

$$K_{dry} = K_0(1-\phi)^{m(\phi)}, \tag{13}$$

$$\mu_{dry} = \mu_0(1-\phi)^{m(\phi)}. \tag{14}$$

Nur et al. (1995) suggested a similar linear modulus-porosity relation with a critical porosity, ϕ_c, which is written as

$$K_{dry} = K_0\left(1 - \frac{\phi}{\phi_c}\right), \tag{15}$$

$$\mu_{dry} = \mu_0\left(1 - \frac{\phi}{\phi_c}\right). \tag{16}$$

The critical porosity for sandstones was found empirically by Nur et al. (1991) to be approximately $\phi_c = 0.40$.

A comparison of the above empirical equations with the numerical data is given in Figure 10. The results are mixed. Neither equation provides a completely satisfactory estimate of the numerically simulated bulk-modulus data over the entire range of porosity. According to both equations (13) and (15), quartz ($K_0 = 37.0$ GPa) and feldspar ($K_0 = 37.5$ GPa), should produce very similar bulk modulus-porosity curves. The numerical data displays considerable deviations between the two mineral systems. Analysis of the numerical shear-modulus data

shows that the Krief equation [equation (14)] provides a very accurate estimate for both mineral systems. The prediction of Nur et al. (1995) for the shear modulus is satisfactory, but does not capture the curvature observed in the numerical data in Figure 10b as well as the Krief model.

The predictions of the Krief et al. (1990) and Nur et al. (1991) models for dry V_p/V_s ratio are poor. Both models assume $[V_p/V_s]_{\text{dry rock}} = [V_p/V_s]_{\text{mineral}}$. This prediction is clearly a poor representation of the numerical data shown in Figure 2d. Arns et al. (2002a) recently studied this limiting behavior of the Poisson's ratio for porous granular models and derived an accurate empirical model for the Poisson's ratio of dry porous materials:

$$\nu_{dry} = a(\phi) + \nu_s\left(1 - \frac{\phi}{\phi_c}\right)^{3/2}, \tag{17}$$

where ν_s is the Poisson's ratio of the mineral phase and $\phi_0 = 1/2$; $a(\phi) = (\phi/\phi_c)^{3/2}/5$, for $\nu_s < 0.2$; and $a(\phi) = 1 - (1 - \phi/\phi_c)^{3/2}/5$, for $\nu_s > 0.2$. The relationship for V_p/V_s is written as

$$V_p/V_s = \sqrt{\frac{\nu - 1}{\nu - 0.5}} = \sqrt{\frac{a(\phi) + \nu_s(1-2\phi)^{3/2} - 1}{a(\phi) + \nu_s(1-2\phi)^{3/2} - 0.5}}. \tag{18}$$

Figure 11 shows a comparison between this empirical model and the numerical data for both ν and for V_p/V_s. The agreement is very good.

Water-saturated rock

Theoretical models.—We compare the theoretical models previously discussed (Hashin-Shtrikman bounds, SCM, DEM, and modified DEM), to our numerical predictions for water

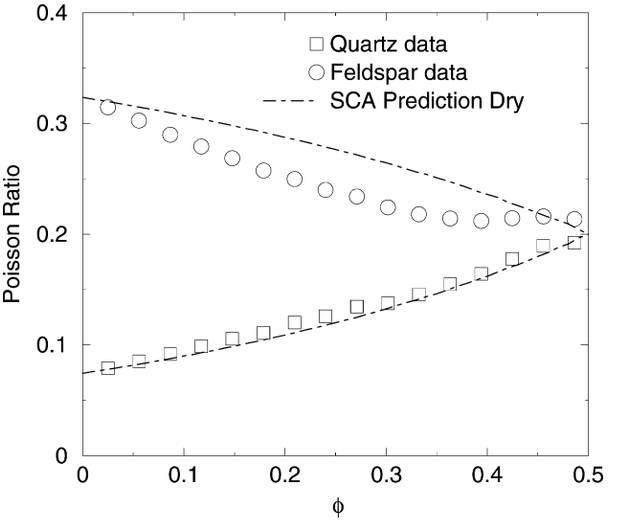

FIG. 9. Comparison of the simulation data to the SCM theory for Poisson's ratio. While the SCM does give the observed limiting behavior, $\nu^*(\phi \to 0.5) \to 0.2$, the prediction of the theory is poor for feldspathic sands.

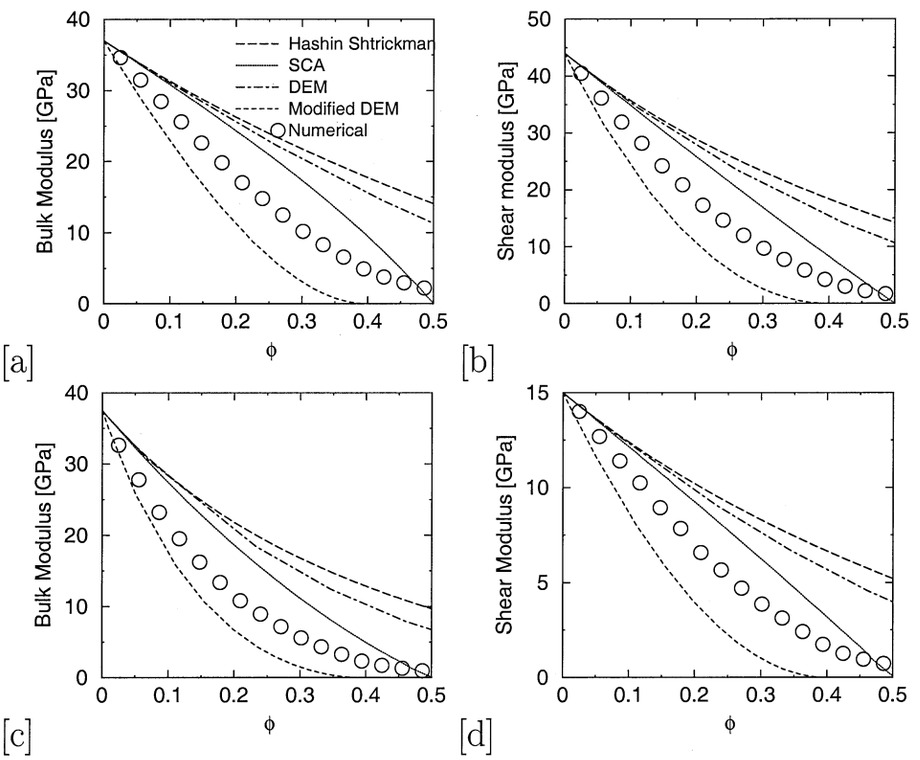

FIG. 8. Comparison of the simulation results to the range of theories used to predict the moduli of dry porous rocks. (a) and (b) give predictions for quartz, (c) and (d) give predictions for feldspar. The Hashin-Shtrikman, SCM, and DEM theories all overestimate the data for all porosities. Of the three, the SCM gives the best theoretical fit to the data as expected from Berge et al. (1993). The modeified DEM underestimates the numerical data.

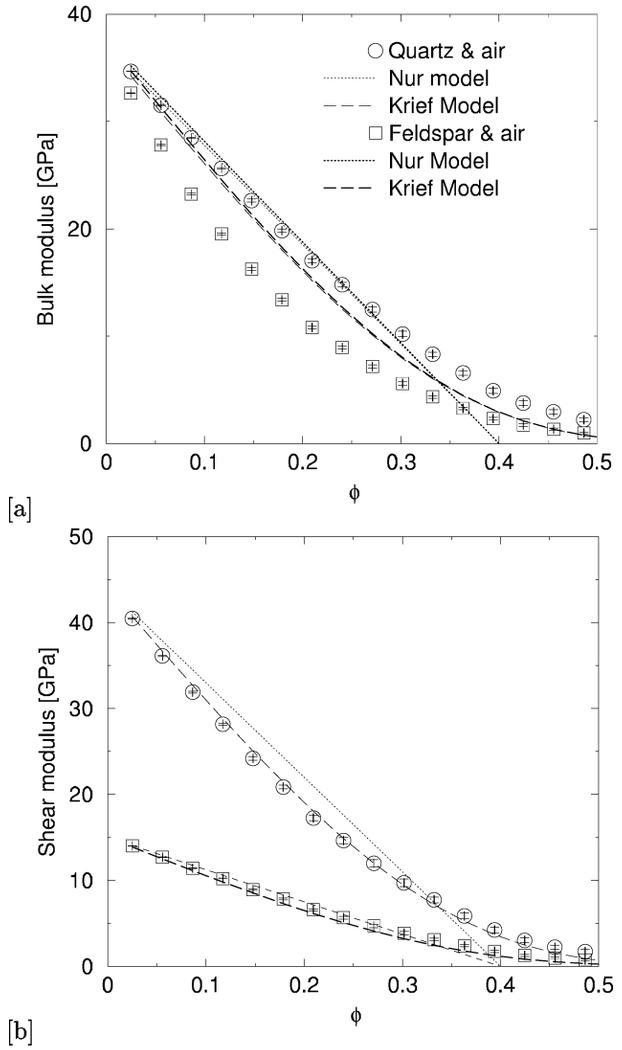

FIG. 10. Comparison of the simulation results on dry monominerallic sandstone microstructures to the empirical models of equations (13) and (14) (Krief et al., 1990) and equations (15) and (16) (Nur et al., 1995). The match to the Krief et al. (1990) model is superior for the shear modulus. Neither model provides a good match to the bulk modulus data.

saturated systems in Figure 12. We note that none of the theoretical models result in a satisfactory fit to the numerical data. Again, the SCM theory provides a much better fit to the data than either the DEM or the Hashin-Shtrikman bounds. This is again consistent with the observations of Berge et al. (1993). Modified DEM underestimates the numerical data.

Empirical models.—As for the dry systems discussed above, relatively simple empirical relationships are often used to estimate the properties of fluid-saturated sedimentary rock. Measurements by Wyllie et al. (1956, 1958, 1963) show that a relatively simple monotonic relationship can describe the relationship between sonic velocity and porosity in saturated sedimentary rocks when mineralogy is relatively uniform. The relationship is written as

$$\frac{1}{V_p} = \frac{\phi}{V_{pf}} + \frac{1-\phi}{V_{ps}}, \tag{19}$$

where V_p, V_{pf}, and V_{ps} are the P-wave sonic velocities of the saturated rock, the pore fluid, and the mineral material, respectively. The interpretation of this expression is that the total transit time is the sum of the transit time of the elastic wave in the mineral and the transit time in the pore fluid. It is therefore often referred to as the time-averaged equation.

Raymer et al. (1980) suggested a number of improvements to Wyllie et al.'s empirical equation relationship. These are summarised by

$$V_p = (1-\phi)^2 V_{ps} + \phi V_{pf}, \phi < 0.37. \tag{20}$$

Figure 13 shows a comparison between numerical data for the OS morphology with the empirical equations of Wyllie et al. (1956, 1958, 1963) and Raymer et al. (1980) for water-saturated quartz and feldspar systems. Overall, the Raymer equation provides a better fit to the numerical data than the Wyllie et al. equation. It estimates the OS morphology velocities to within 10% error for quartz sands and 2–3% for feldspathic sands.

Nur et al. (1991, 1995) postulated that the moduli of saturated rocks should trend in a similar manner to that predicted by equations (15)–(16) for dry rocks. Accordingly, the moduli for saturated systems should trend linearly betweeen the mineral grain modulus at low porosity to a value for a mineral-fluid suspension at the critical porosity. Figure 14 shows a comparison between the Nur et al. (1991, 1995) model and the

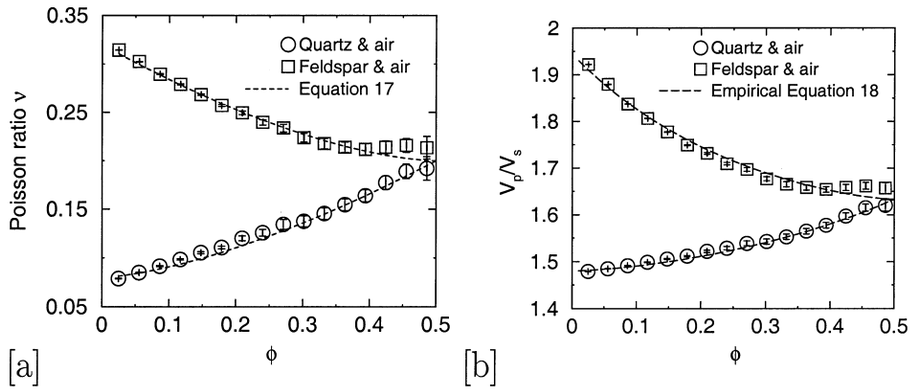

FIG. 11. Comparison of the simulation results on dry monominerallic sandstone microstructures to the empirical model of Arns et al. (2002a) given in equation (17)–(18). Agreement is excellent.

numerical data for the quartz and feldspar systems. The results are mixed. The model provides reasonable estimates of the numerical data for the bulk modulus of the quartz system, but the corresponding estimates for feldspar are poor. The model clearly fails to account for the strong effect of mineralogy exhibited by the numerical data. In comparison with the bulk modulus predictions, the prediction for the shear modulus is satisfactory for feldspathic sands, but poor for the quartz system.

PROPOSED VELOCITY-POROSITY MODEL FOR CLEAN SANDSTONES

On the basis of the numerical simulations on the OS morphology and the comparisons with existing models and theories discussed above, we propose a new empirical method for accurately estimating the full velocity-porosity relationship for monomineralic consolidated sands from only a knowledge of the mineral modulus. The method is based on the excellent match to the numerical data of both the empirical Krief

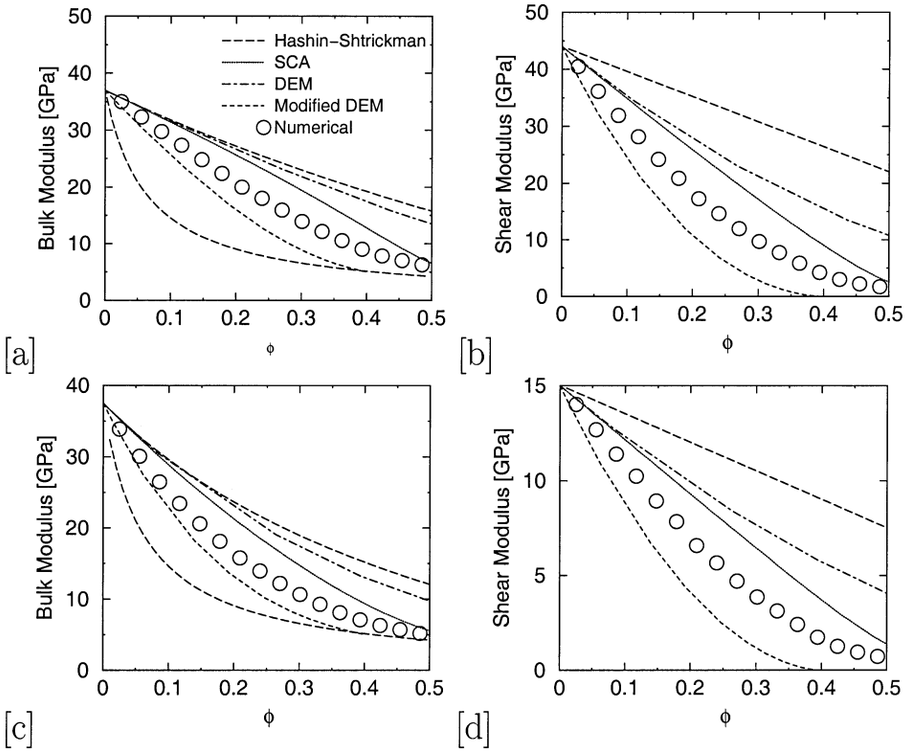

FIG. 12. Comparison of the simulation results to the range of theories used to predict the moduli of water saturated rock. (a) and (b) give predictions for quartz, (c) and (d) give predictions for feldspar. The Hashin-Shtrikman bounds are quite broad for the bulk modulus, and neither bound is predictive. The lower bound is zero for the shear modulus. The SCM and DEM both overestimate the data for all porosities. The SCM gives the best theoretical fit to the data as expected from Berge et al. (1993).

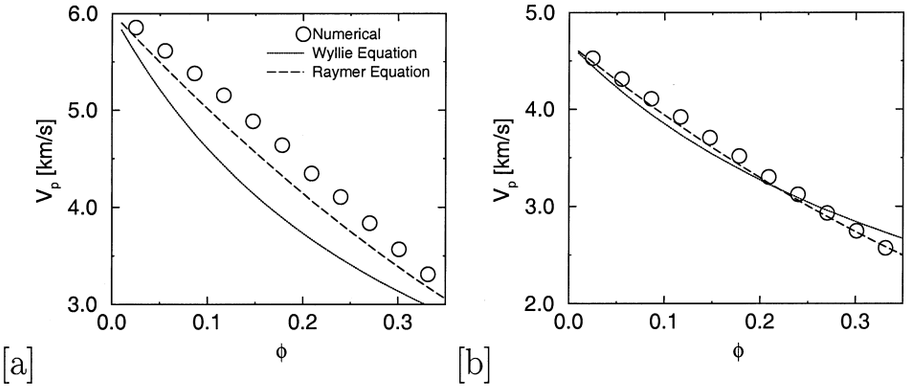

FIG. 13. Comparison of the results of the simulations for water-saturated (a) quartz and (b) feldspathic sands to the empirical equations of Wyllie et al. [equation (19)] and Raymer [equation (20)]. The Raymer equation is satisfactory and gives a better prediction than the Wyllie et al. equation. The prediction of the Raymer equation is particularly excellent for feldspathic sands.

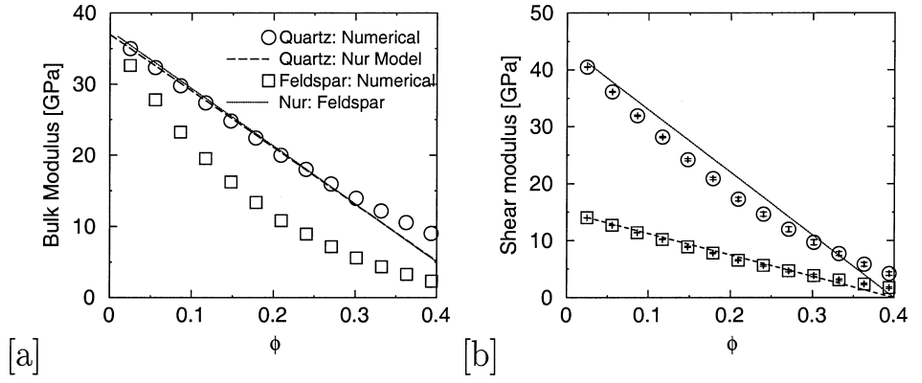

FIG. 14. Comparison of the results of the simulations for water-saturated (a) quartz and (b) feldspar sands to the empirical equation of (Nur et al., 1995). For the bulk modulus, the model accurately describes the quartzose sands but not the feldspathic sands. For the shear modulus, the feldspathic sand is best matched.

equation for the shear modulus of a dry sandstone and the empirical equation of Arns et al. (2002b) for the Poisson's ratio of a dry porous rock:

$$\mu_{dry}(\phi) = \mu_s(1-\phi)^{m(\phi)}, \tag{21}$$

$$\nu_{dry} = a(\phi) + \nu_s(1-\phi/\phi_c)^{3/2}, \tag{22}$$

where μ_s and ν_s are the shear modulus and Poisson's ratio, respectively, for the pure solid mineral phase; $m(\phi) = 3/(1-\phi)$ and $a(\phi) = (\phi/\phi_c)^{3/2}/5$, for $\nu_s < 0.2$; and $a(\phi) = 1-(1-\phi/\phi_c)^{3/2}/5$, for $\nu_s > 0.2$. Gassmann's equations are subsequently used to predict the saturated states for any fluid.

We compare the predictions of the proposed empirical model to the numerical data discussed above and to the empirical critical porosity model of Nur et al. (1991, 1995) [equations (15)–(16)]. Results of the comparisons are summarized in Figure 15. The proposed empirical method is in excellent agreement with the numerical data for all the calculated elastic properties, both for dry and water-saturated systems. The method appears to be superior to the critical porosity model. For porosities $\phi < 35\%$, the method predicts modulus values, which are within 2% error for the dry case and 5% error for the water-saturated case.

Figure 16 shows a comparison between the proposed empirical method, the critical porosity model, and the experimental data of Han (1986), together with the dry and water-saturated velocity-porosity relationships derived from experimental data by Han (1986) for clean sandstones. The agreement between the proposed empirical method and the experimental data of Han (1986) is encouraging.

CONCLUSIONS

1) The OS model is used to describe the microstructure of clean sandstones. Numerical predictions of elastic properties based on this model are in good agreement with available experimental data for clean quartzose sandstones for both dry and water-saturated states.
2) The data sets generated by numerical simulations on the OS morphology have been shown to be markedly less noisy or scattered than corresponding experimental measurements. The almost total absence of noise has allowed us to quantitatively compare model-generated numerical data with available theoretical models and empirical equations. The numerical data is also shown to be in good agreement with the analytical Gassmann's relations.
3) The comparisons show that the common theoretical models (bounds and effective medium theories) for both dry and water-saturated states are not particularly accurate (Figures 8 and 12). The models significantly overestimate modulus data as a function of porosity ϕ. The SCM predictions for ν (or V_p/V_s) do, however, show the correct limiting behaviour for large ϕ (Figure 9).
4) Comparisons with a number of dry modulus-porosity models show that the bulk modulus-porosity relationships of both Krief et al. (1990) and Nur et al. (1995) fail to accurately describe the numerical data (Figure 10a). However, the Krief equation [equation (14)] does provide a very good match for the dry shear modulus data with <2% error (Figure 10b). An accurate empirical ν-ϕ or V_p/V_s-ϕ [equations (17) or (18)] relationship for dry sandstone also matches the numerical data very well (Figure 11).
5) The Raymer equation [equation (20)] is the best of the modulus-porosity models for this model morphology of well-consolidated sands under water-saturated conditions. Errors of less than 10% are observed across the full range of ϕ (Figure 13). The critical porosity model of Nur et al. (1991, 1995) results in a poor fit to the numerical data for K_{sat} versus ϕ, but a satisfactory fit to μ_{sat} versus ϕ (Figure 14).
6) Based on our numerical data for clean consolidated systems, we propose that the modulus-porosity relations may be accurately estimated for clean cemented sands using the empirical Krief equation for the shear modulus of a dry sandstone and the empirical equation of Arns et al. (2002a) for the Poisson's ratio of a dry porous rock. Gassmann's equations can then be used to predict the fluid-saturated states. The results of comparisons of the method to numerical model data and available experimental data are encouraging.

REFERENCES

Arns, C. H., Knackstedt, M. A., and Pinczewski, W. V., 2002a, Accurate $V_p : V_s$ relationships for dry consolidated sandstones: Geophys. Res. Lett., **29**, art. 1202.
Arns, C. H., Knackstedt, M. A., Pinczewski, W. V., and Garboczi, E. J., 2002b, Computation of linear elastic properties from

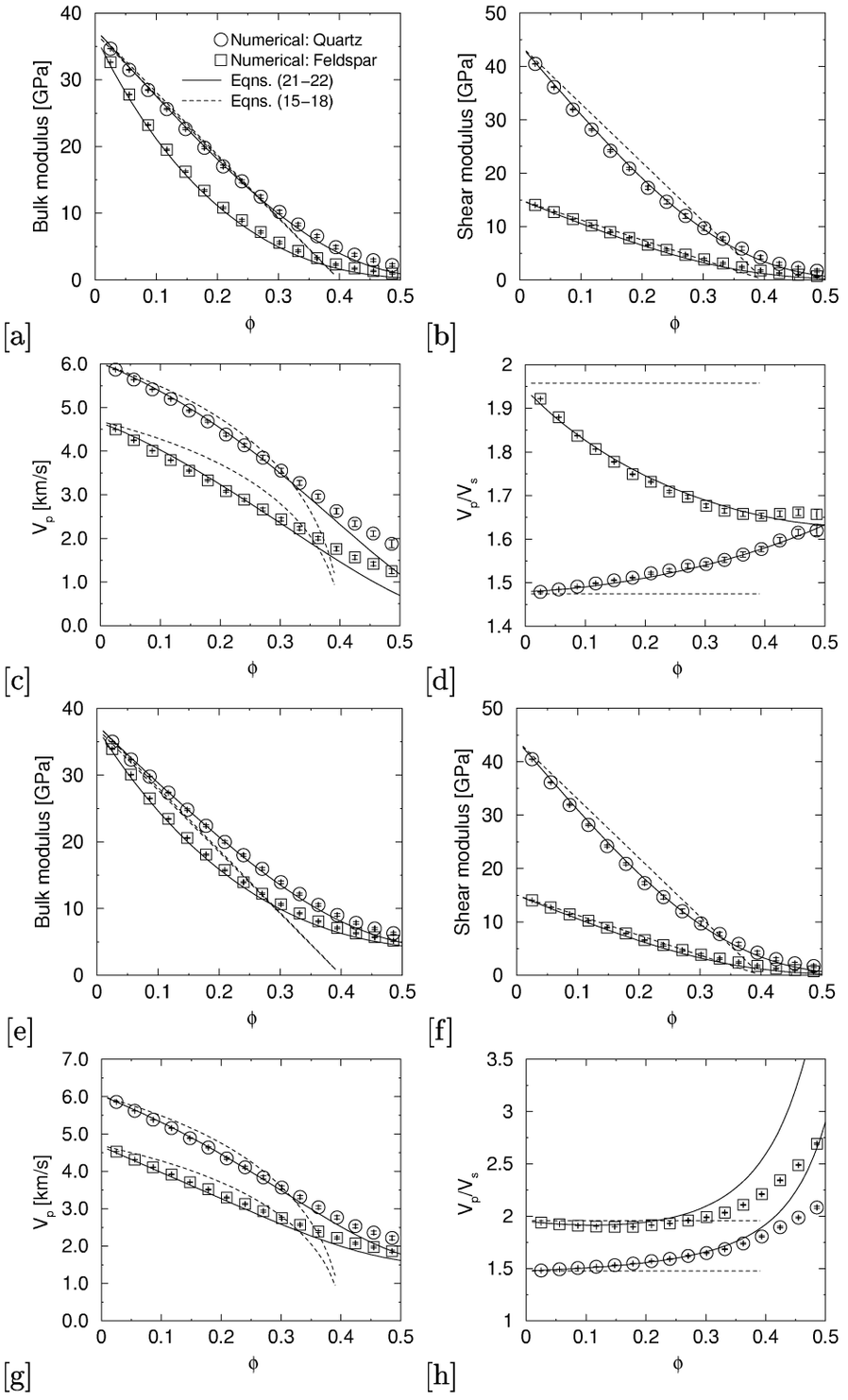

FIG. 15. Comparison of the prediction of the proposed empirical model [equations (21)–(22)] and the critical porosity model [equations (15)–(16)] to the simulation results for dry (a) bulk modulus, (b) shear modulus, (c) V_p, and (d) V_p/V_s ratio as a function of porosity for the single phase OS model with quartz and feldspar as the mineral phase. (e)–(h) give the predictions for the water-saturated case derived from the dry data using Gassmann's relations.

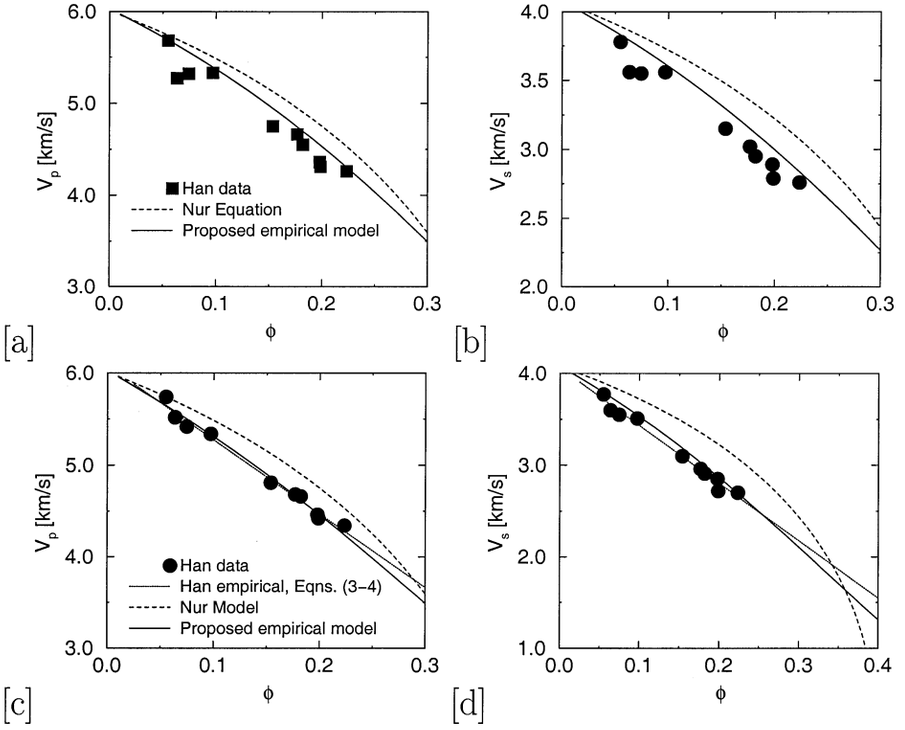

FIG. 16. Comparison of the prediction of the proposed empirical equations (21)–(22) and the critical porosity model (Nur et al., 1995) to the experimental data (Han, 1986) for clean dry quartz sands (a)–(b) and clean water-saturated sands (c)–(d). (c)–(d), we give the empirical velocity-porosity fit for the clean water-saturated sands derived by Han from the experimental data.

microtomographic images: Methodology and agreement between theory and experiment: Geophysics, **67**, 1396–1405.
Berge, P. A., Berryman, J. G., and Bonner, B. P., 1993, Influence of microstructure on rock elastic properties: Geophys. Res. Lett., **20**, 2619–2622.
Berryman, J. G., 1980, Long-wavelength propagation in composite elastic media: J. Acous. Soc. Am., **69**, 416–424.
——— 1992, Single-scattering approximations for coefficients in Biot's equations of poroelasticity: J. Acoust. Soc. Am., **91**, 551–571.
Budiansky, B., 1965, On the elastic moduli of some heterogeneous materials: J. Mech. Phys. Solids, **13**, 223–227.
Castagna, J. P., Batzle, M. L., and Kan, T. K., 1993, Rock physics—The link between rock properties and AVO response, *in* Castagna, J. P., and Backus, M. M., Eds., Offset-dependent reflectivity—Theory and practice of AVO analysis:: Soc. Expl. Geophys., 135–171.
Day, A. R., Snyder, K. A., Garboczi, E. J., and Thorpe, M. F., 1992, The elastic moduli of a sheet containing circular holes: J. Mech. and Phys. of Solids, **40**, 1031–1051.
Garboczi, E. J., 1998, Finite element and finite difference programs for computing the linear electric and linear elastic properties of digital images of random materials: National Institute of Standards and Technology Internal Report 6269.
Garboczi, E. J., and Day, A. R., 1995, An algorithm for computing the effective linear elastic properties of heterogeneous materials: Three-dimensional results for composites with equal phase Poisson ratios: J. Mech. Phys. Solids, **43**, 1349–1362.
Gubernatis, J., and Krumsahl, J., 1975, Macroscopic engineering properties of polycrystalline materials: J. Appl. Phys., **46**, 1875–1883.
Han, D.-H., 1986, Effects of porosity and clay content on acoustic properties of sandstones and unconsolidated sediments: Ph.D. diss., Stanford University.
Hashin, Z., 1983, Analysis of composite materials: A survey: J. Appl. Mech., **50**, 481–505.
Hashin, Z., and Shtrikman, S., 1962, A variational approach to the theory of the effective magnetic permeability of multiphase materials: J. Appl. Phys., **33**, 3125–3131.
——— 1963, A variational approach to the elastic behaviour of multiphase materials: J. Mech. Phys. Solids, **11**, 127–140.
Hill, R., 1965, A self-consistent mechanics of composite materials: J. Mech. Phys. Solids, **13**, 213–222.
Korringa, J., Brown, R., thompson, D., and Runge, R., 1979, Self consistent imbedding and the ellipsoidal model for porous rocks: J. Geophys. Res., **84**, 5591–5598.
Krief, M., Garat, J., Stellingwerff, J., and Ventre, J., 1990, A petrophysical interpretation using the velocities of P and S waves (full waveform sonic): The Log Analyst, **31**, 355–369.
Marion, D., Nur, A., Yin, H., and Han, D., 1992, Compressional velocity and porosity in sand-clay mixtures: Geophysics, **57**, 554–563.
Mavko, G., Mukerji, T., and Dvorkin, J., 1998, The rock physics handbook: Cambridge University Press.
Milton, G. W., 1982, Bounds on the elastic and transport properties of two-component composites: J. Mech. Phys. Solids, **30**, 177–191.
Mukerji, T., Berryman, J., Mavko, G., and Berge, P., 1995, Differential effective medium modeling of rock elastic moduli with critical porosity constraints: Geophys. Res. Lett., **22**, 555–558.
Nur, A., Marion, D., and Yin, H., 1991, Wave velocities in sediments, *in* Hovem, J., Richardson, M. D., and Stoll, R. D., Eds., Shear waves in marine sediments: Kluwer Academic, Press, 131–140.
Nur, A., Mavko, G., Dvorkin, J., and Galmundi, D., 1995, Critical porosity: The key to relating physical properties to porosity in rocks: 65th Ann Internat. Mtg., Soc. Expl. Geophys., Expanded Abstracts 878.
Øren, P. E., Bakke, S., and Arntzen, O. J., 1998, Extending predictive capabilities to network models: Soc. Petr. Eng. J., **3**, 324–336.
Pickett, G. R., 1963, Acoustic character logs and their applications in formation evaluation: J. Petr Tech., **15**, 650–667.
Raymer, L. L., Hunt, E. R., and Gardner, J. S., 1980, An improved sonic transit time to porosity transform: 21st Ann. Logging Symp., Soc. Prof. Well Log Analysts, Trans., Paper P.
Roberts, A. P., and Garboczi, E. J., 2000, Elastic properties of model porous ceramics: J. Am. Ceramic Soc., **83**, 3041–3048.
Thovert, J.-F., Yousefian, F., Spanne, P., Jacquin, C. G., and Adler, P. M., 2001, Grain reconstruction of porous media: Application to a low-porosity Fontainebleau sandstone: Phys. Rev. E, **63**, 061307.
Wyllie, M., Gregory, A., and Gardner, G., 1956, Elastic wave velocities in heterogeneous and porous media: Geophysics, **21**, 41–70.
——— 1958, An experimental investigation of factors affecting elastic wave velocities in porous media: Geophysics, **23**, 459–493.
Wyllie, M., Gardner, G., and Gregory, A., 1963, Studies of elastic wave attenuation in porous media: Geophysics, **27**, 569–589.